

11-1-1998

Detection of Silver in Metal-Poor Stars

James L. Crawford
University of Texas

Christopher Sneden
University of Texas

Jeremy R. King
Clemson University, jking2@clemson.edu

Ann M. Boesgaard
University of Hawaii

Contantine P. Deliyannis
Indiana University

Follow this and additional works at: https://tigerprints.clemson.edu/physastro_pubs

Recommended Citation

Please use publisher's recommended citation.

This Article is brought to you for free and open access by the Physics and Astronomy at TigerPrints. It has been accepted for inclusion in Publications by an authorized administrator of TigerPrints. For more information, please contact kokeefe@clemson.edu.

DETECTION OF SILVER IN METAL-POOR STARS

JAMES L. CRAWFORD AND CHRISTOPHER SNEDEN

Department of Astronomy and McDonald Observatory, University of Texas, RLM 15.308, Austin, TX 78712; jocco@astro.as.utexas.edu, chris@verdi.as.utexas.edu

JEREMY R. KING¹

Space Telescope Science Institute, 3700 San Martin Drive, Baltimore, MD 21218; jking@stsci.edu

ANN M. BOESGAARD¹

Institute for Astronomy, University of Hawaii, 2680 Woodlawn Drive, Honolulu, HI 96822; boes@galileo.ifa.hawaii.edu

AND

CONSTANTINE P. DELIYANNIS¹

Department of Astronomy, Indiana University, 319 Swain Hall West, Bloomington, IN 47405; con@athena.astro.indiana.edu

Received 1998 May 13; revised 1998 August 6

ABSTRACT

The resonance lines of neutral silver appearing at 3280, 3382 Å in the near-ultraviolet spectral region have been identified on Keck I HIRES spectra of four halo stars with metallicities $-1.3 \geq [\text{Fe}/\text{H}] \geq -2.2$. This represents the first detection in metal-poor stars of an element in the atomic number range $41 \leq Z \leq 55$. The mean relative silver abundance is $\langle [\text{Ag}/\text{Fe}] \rangle \simeq +0.2$, with little star-to-star variation. Silver abundance upper limits in three other metal-poor stars are consistent with this mean value. The modest overabundance of silver is similar to the overabundances in this metallicity range exhibited by other neutron-capture elements whose primary nucleosynthesis origin is the r -process (such as europium and dysprosium).

Key words: Galaxy: halo — stars: abundances — stars: Population II

1. INTRODUCTION

The majority of elements in the periodic table are synthesized in reaction chains comprising captures of free neutrons by target nuclei and subsequent β -decays. Neutron-capture elements are those with $Z > 30$, and their isotopes are generally created in two kinds of neutron bombardment environments. If the neutron flux is sufficiently low, unstable nuclei will undergo β -decays between successive neutron captures, and the element buildup will proceed along the “valley of β -stability”; this is called the s -process. Very large neutron fluxes, on the other hand, will saturate target nuclei out to the “neutron-drip line,” and then β -decays will quickly restabilize these heavier nuclei in the direction of the β -stability line; this is called the r -process. Recent reviews of the r -process and s -process have been given by Meyer (1994) and Wallerstein et al. (1997), among others. Most s -process nucleosynthesis apparently occurs during the shell helium burning phase of low- to medium-mass stars, while the r -process probably happens during Type II supernovae (SNe; see, e.g., Cowan, Thielemann, & Truran 1991).

Solar system neutron-capture element abundances are due to both r - and s -processes. Käppeler, Beer, & Wisshak (1989) have published the most recent comprehensive review of the relative contributions of each process to individual isotopes in primordial solar system material. However, division of neutron-capture nucleosynthesis into just these two processes is probably an oversimplification. For example, at least two distinct s -processes are needed to

adequately match solar system isotopic abundances (see, e.g., Käppeler et al.). In addition, in considering the discrepancy between the inferred abundances of certain r -process isotopes in the early solar system and their expected steady state values in the interstellar medium, Wasserburg, Busso, & Gallino (1996) suggest that “there are distinctive SN sources for different r -process nuclei with a sharp distinction in different SN contributions below and above $A \sim 140$.”²

For the most metal-poor halo stars, studies spanning several decades (summarized by McWilliam 1997 and Wallerstein et al. 1997) have concluded that the abundance ratios of the spectroscopically accessible neutron-capture elements are well matched to the solar system r -process abundance fractions; an s -process component is weak or absent. This is in general accord with the expected dominance of high mass star SNe nucleosynthesis in the early Galaxy. But except for a few stars that fortuitously display many neutron-capture element features (e.g., CS 22892-052; Sneden et al. 1996), in most low-metallicity stars the assertion of r -process dominance has been based primarily on the abundances of very few elements. A popular r -/ s -marker is the ratio of Ba (synthesized most efficiently in the s -process) to Eu (almost exclusively a product of the r -process). Also, the abundance level of the Sr \rightarrow Zr element group to the Ba \rightarrow Eu group is used to clarify the synthesis efficiencies of elements near the first and second “neutron-capture abundance peaks.”

¹ Visiting Astronomer, W. M. Keck Observatory, which is jointly operated by the California Institute of Technology and the University of California.

² Nuclei with mass numbers $A \sim 140$ are just beyond the second neutron-capture abundance peak, and these have atomic numbers of $Z \sim 57$. Thus the Wasserburg et al. proposed split in the efficiencies of their two r -processes occurs near La, the least massive of the rare earth elements.

Direct confrontation of neutron-capture synthesis theories can come only from determination of abundances of many elements over the full $Z > 30$ range. Many neutron-capture elements (for example, the noble gas Xe) will probably never be detected in cool metal-poor stars, because of the lack of any strong transitions in the spectra of these stars. However, other neutron-capture elements have not been studied simply because their strong transitions occur either in the vacuum ultraviolet ($\lambda < 3000 \text{ \AA}$) or in the inconvenient ultraviolet ($3000 \text{ \AA} < \lambda < 3700 \text{ \AA}$), where stellar fluxes are low, telluric opacity increases rapidly toward shorter wavelengths, and spectrograph efficiencies are often small. In fact, only two very metal-poor stars, HD 122563 and CS 22892-052, have had extensive exploration of their spectrum below 4000 \AA (Wolff & Wallerstein 1967; Sneden & Parthasarathy 1983; Sneden et al. 1996). Fortunately, the observational situation is changing. With the *Hubble Space Telescope's* GHRS and STIS and efficient high-resolution spectrographs attached to the new 10 m-class telescopes, the UV spectral region is opening up to stellar abundance studies.

In this paper we analyze the neutral silver resonance lines appearing on Keck I HIRES spectra of several metal-poor stars. In so doing, Ag ($Z = 47$) becomes the first element in the $41 \leq Z \leq 55$ gap between Zr and Ba to be detected in metal-poor stars. In addition, Ag has potential importance in the discussions of r - and s -process balance in early Galactic nucleosynthesis. We will show here that, down to metallicities³ of $[\text{Fe}/\text{H}] \simeq -2.2$, $\langle [\text{Ag}/\text{Fe}] \rangle \simeq 0.2$ and there are no obvious trends in this abundance with metallicity.

2. OBSERVATIONS AND DATA REDUCTION

We obtained spectra of four cool metal-poor stars using the HIRES echelle spectrograph (Vogt et al. 1994) on the Keck I 10 m telescope as part of an ongoing program to determine stellar beryllium abundances from the near-UV $\lambda 3130 \text{ Be II}$ resonance features (Boesgaard 1996). These spectra cover the approximate wavelength range $3050\text{--}3400 \text{ \AA}$; this part of the spectrum contains useful features of several interesting heavy metals with which to derive abundances. The UT dates of the observations, number of individual exposures, total exposure time, and the approximate Poisson-based signal-to-noise ratio (S/N) per (continuum) pixel at the wavelengths of interest here ($\lambda \sim 3300 \text{ \AA}$) are summarized in Table 1.

Preliminary processing (overscan subtraction, debiasing, and trimming) was performed with standard IRAF⁴ routines. Initial-order identification, tracing, and flat-fielding were carried out with the specialized suite of FIGARO echelle reduction routines, developed and modified by J. McCarthy and A. Tomaney, imported into the IRAF environment at the University of Texas. Scattered-light cor-

TABLE 1
OBSERVATIONAL DATA

Star	Date (UT)	N_{exp}	t_{tot} (s)	S/N (pixel ⁻¹)
HD 2665	1995 Oct 27	2	3000	195
HD 6755	1995 Oct 27	2	3600	225
HD 24289	1994 Oct 26	3	12600	115
HD 84937	1994 Mar 1	3	2700	175
HD 103095	1994 Apr 28	3	900	165
HD 140283	1994 Mar 1	3	3600	305
BD +37° 1458	1995 Mar 15	2	4500	175

rections, final-order tracing, one-dimensional extraction, and dispersion solutions were conducted using nominal IRAF echelle package routines. The linearized dispersion in the wavelength regions of interest is $\sim 0.022 \text{ \AA pixel}^{-1}$. The 3.2 pixel FWHM of ThAr lamp spectra gives a measured inverse instrumental resolving power of $R \sim 45,000$. We accomplished subsequent co-addition of the individual spectra, (pseudo-) continuum rectification, and other rudimentary manipulations with the specialized single spectral order software package SPECTRE (Fitzpatrick & Sneden 1987).

3. ANALYSIS

3.1. Identification of Ag I Resonance Lines

The solar photospheric abundance of silver is based entirely upon Ross & Aller's (1972) analysis of the strong Ag I resonance lines at $3280.7, 3382.9 \text{ \AA}$. The equivalent widths of these lines in the solar center-of-disk spectrum are 44 and 22 m\AA , according to Moore, Minnaert, & Houtgast (1966). Ross & Aller derived $\log \epsilon(\text{Ag}) = 0.85$, which was later corrected by Grevesse (1984) to $\log \epsilon(\text{Ag}) = 0.94$ with a recommended uncertainty of ± 0.25 , and this value has not changed since then (Grevesse, Noels, & Sauval 1996). Frustratingly, the recommended solar system meteoritic abundance has also remained steady at $\log \epsilon(\text{Ag}) = 1.24 \pm 0.01$, a factor of 2 larger. This clash between photospheric and meteoritic silver abundances, one of the rare significant disagreements between these two abundance sets, remains unresolved at this time.

Since the near-UV Ag I lines arise from the ground state, they should retain reasonable strengths in cooler stars at substantially subsolar metallicities. Preliminary reconnaissance of our spectra revealed their presence in the four coolest stars, but not in the three warmer (and very metal-poor) ones. In Figure 1 we display the $\lambda 3280$ spectra of all stars to illustrate this point. The figure also shows that this Ag I line, like the $\lambda 3382$ line, is blended by other atomic transitions, and an abundance analysis must be done via synthetic spectrum computations.

We also searched our spectra for transitions of other elements near silver in the periodic table. Lines of palladium ($Z = 46$) and cadmium ($Z = 48$) are known to exist in this spectral region. Moore et al. (1966) identified Pd I at 3242.71 \AA , with an equivalent width of 26 m\AA in the solar spectrum. A feature at that wavelength appears in the stronger lined stars of our sample. However, there appears to be strong contamination of the Pd I line by an OH line, and test synthetic spectrum computations demonstrated that derivation of trustworthy palladium abundances from this

³ We adopt the usual spectroscopic notations that $[A/B] \equiv \log(N_A/N_B)_{\text{star}} - \log(N_A/N_B)_{\odot}$ and that $\log \epsilon(A) \equiv \log(N_A/N_H) + 12.0$, for elements A and B. Also, metallicity is arbitrarily defined as the stellar $[\text{Fe}/\text{H}]$ value.

⁴ IRAF is distributed by the National Optical Astronomical Observatories, which are operated by the Association for Universities for Research in Astronomy, Inc., under cooperative agreement with the National Science Foundation.

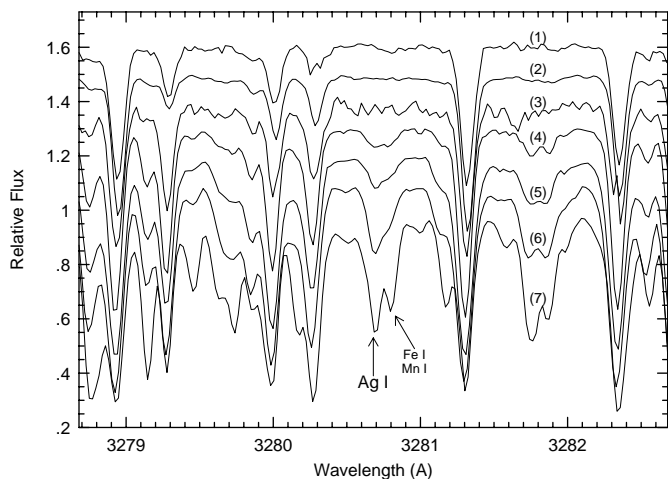


FIG. 1.—Observed spectra surrounding the Ag I resonance line at 3280.7 Å in the seven metal-poor stars considered in this study. The stars, from top to bottom in the figure, are (1) HD 84937, (2) HD 140283, (3) HD 24289, (4) BD +37°1458, (5) HD 2665, (6) HD 6755, and (7) HD 103095. Detections of the Ag I feature are seen in the bottom four spectra.

feature would be quite difficult. The same OH blending problem also frustrated our attempts to analyze the Cd I at 3261.06 Å (23 mÅ in the solar spectrum according to Moore et al.). No features of any other element in the atomic number range $41 \leq Z \leq 55$ could be easily detected on our spectra, and therefore all subsequent discussion will concentrate exclusively on Ag.

3.2. Derivation of Line Lists and the Solar Silver Abundance

The LTE line analysis code MOOG (Sneden 1973) was employed to generate synthetic spectra of the wavelength regions surrounding the Ag I features. The initial line lists for the synthetic spectra were taken from R. L. Kurucz's compilations of atomic and molecular lines (see, e.g., Kurucz & Peytremann 1975; Kurucz 1995a, 1995b); the relevant molecules in the spectral regions of interest are OH and NH. To refine our initial line lists in each spectral region, we generated synthetic solar spectra with these lists and the Holweger & Müller (1974) solar model atmosphere and compared these spectra with the Solar Flux Atlas of Kurucz et al. (1984). Through these comparisons we adjusted the line lists by (a) making small corrections to an individual line's wavelength; (b) changing the gf -value of a specific line; and (c) on a few occasions, adding a line (arbitrarily defined to be an Fe I line with excitation potential $EP = 2.5$ eV) to take the place of an unidentified line in the solar spectrum. In this exercise, we made extensive use of the Moore et al. (1966) solar atlas to aid line identification and placement of unidentified lines.

The transition probabilities for the Ag I resonance lines have been measured in several laboratory studies, and therefore we adopted without change the values recommended in Fuhr & Wiese's (1996) "critical compilation": $\log gf(3280 \text{ Å}) = 0.044$, and $\log gf(3382 \text{ Å}) = 0.350$. These lines have significant hyperfine splitting, but fortunately the component wavelengths and relative strengths are well known; we adopted the substructure parameters given in Table 3 of Ross & Aller (1972). Both Ag I lines are blended with transitions of other species. Specifically, near the 3280.68 line there is contamination by Fe I λ 3280.76 and Mn I λ 3280.76 (as noted by Ross & Aller 1972), and possibly

a small contribution from NH 3280.76 Å. Close to Ag I λ 3382.90 the dominant contaminant is Fe I λ 3382.99, but it is reasonably well resolved from the Ag I line. The Fe I line was absent in the initial line list, but is identified in the solar spectrum by Moore et al. (1966), so we added it to the line list and iterated its gf -value in the manner described above. The entire 3383 Å region is polluted by numerous weak NH lines, including one at 3382.87 Å, which has a strength roughly 10% the total Ag I line strength in the solar spectrum.

Using the iterated line lists we estimated $\log \epsilon(\text{Ag}) = 1.10 \pm 0.05$ and 1.05 ± 0.05 from the 3280 and 3382 Å lines, respectively. The quoted uncertainties given here are estimates of the combined effects of continuum placement and line profile fitting errors. Note that although the 3280 Å line is a factor of 2 stronger than the 3382 Å line, it also is more blended with other species transitions, limiting the accuracy of its derived abundance. The mean derived solar abundance is $\log \epsilon = 1.08 \pm 0.08$, where the total uncertainty reflects both the individual abundance uncertainties from each line and the difference in derived abundance between them. Tests using a Kurucz (1993) or MARCS (Gustafsson et al. 1975) model solar atmosphere resulted in mean Ag abundances of about 0.10 dex less than the value determined with the Holweger-Müller (1974) model. We adopt here the Ag abundance derived with the Holweger-Müller solar model, since for most other species it yields photospheric abundances in excellent agreement with meteoritic abundances (e.g., Hannaford et al. 1982 and references therein). We also note that since our program stars are so different in metallicity than the Sun (most are very different in T_{eff} and $\log g$ also), it is not clear that use of the Holweger-Müller empirical model for the Sun and Kurucz models for the stars is inherently less trustworthy than the use of Kurucz (or MARCS) models throughout.

Our recommended solar photospheric Ag abundance, $\log \epsilon = 1.08 \pm 0.08$, is low compared with the meteoritic abundance ($\log \epsilon = 1.24$; Grevesse et al. 1996), but it halves the gap in $\log \epsilon$ from Ross & Aller's (1972) value of 0.94. It is possible to reconcile our photospheric abundance with the meteoritic value by an arbitrary addition of extra "continuum" opacity. Balachandran & Bell (1997, 1998) argue that an opacity increase by a factor of ~ 1.6 near 3130 Å can solve a similar disagreement between photospheric and meteoritic beryllium abundances. Simple numerical experiments here suggest that the needed extra opacity at 3280 Å is a factor of ~ 1.3 . This is not a very large "missing" opacity factor for a spectral region with many remaining questions about opacity sources, but little weight should be attached to the exact value of the opacity factor suggested by the numerical tests here. A definitive study of the solar Ag abundance is beyond the scope of this work, and the reader must keep in mind that scale uncertainties of the order of 0.1 dex remain associated with the solar analysis of this element. These scale errors affect the absolute values of the [Ag/Fe] ratios derived here but should not obscure any trends with [Fe/H].

3.3. Stellar Silver Abundances

We adopted the model stellar atmosphere parameters derived by Deliyannis et al. (1998), or followed their precepts in estimating the parameters for stars not analyzed by them; here we briefly summarize their work. To begin, $b - y$, $B - V$, $V - K$, and $R - I$ photometry was used to

TABLE 2
MODELS AND SILVER ABUNDANCES

Star	T_{eff} (K)	$\log g$	v_t (km s^{-1})	[M/H] Model	[Fe/H] 3280 Å	[Fe/H] 3382 Å	[Ag/Fe] 3280 Å	[Ag/Fe] 3382 Å
HD 2665	4978	2.35	1.3	-2.00	-1.90	-2.00	-0.12	+0.10
HD 6755	5212	3.14	1.3	-1.60	-1.50	-1.70	+0.23	+0.50
HD 24289	5800	4.00	1.0	-2.20	-2.20	...	< +0.5	...
HD 84937	6206	3.89	1.5	-2.20	-2.20	...	< +0.2	...
HD 103095	5007	4.65	1.5	-1.37	-1.27	-1.37	+0.25	+0.30
HD 140283	5692	3.47	1.5	-2.56	-2.46	-2.46	< +2.6	< +2.1
BD +37° 1458	5300	3.30	1.5	-2.20	-2.15	...	+0.19	...

determine T_{eff} values, based on the color- T_{eff} relations of Carney (1983) and King (1993). Initial [Fe/H] values were taken from high-quality modern literature studies; these estimates were adjusted to reflect the differing T_{eff} choices of the individual studies and then averaged. Gravities were estimated via two methods. First, $\log g$ values were taken from literature model atmosphere analyses (which employed ionization balance conditions), and these were adjusted to account for any difference between the T_{eff} values employed in those studies and those adopted here. Second, $\log g$ was also calculated from the stars' position in the $\log g$ versus T_{eff} plane of a $Y = 0.24$, 17 Gyr Revised Yale Isochrone (Green, Demarque, & King 1987). The two $\log g$ estimates were averaged.

The stars HD 24289 and BD +37°1458 were not considered by Deliyannis et al. (1998). For HD 24289, our adopted T_{eff} and [M/H] values are nearly identical to those employed by Ryan et al. (1996), and we assumed $\log g = 4.0$ in the absence of a literature gravity estimate. For BD +37°1458, we adopted the T_{eff} recommended by Pilachowski, Sneden, & Booth (1993), $\log g = 3.3$, which is consistent with determinations by Fuhrmann, Axer, & Gehren (1995) and Tomkin et al. (1992); we adopted a metallicity [M/H] = -2.2 that is a compromise of a large range of literature estimates. The microturbulent velocities of 1.0 km s^{-1} for HD 24289 and 1.5 km s^{-1} for BD +37°1458 are approximations for values appropriate to stars of their respective gravities.

These parameters were then used to interpolate in the Kurucz (1993) grid of ATLAS models to produce the desired models for each star. Deliyannis et al. (1998) investigate Be abundances using two different effective temperature scales: a "low" scale in good agreement with most published abundance investigations, and a "high" scale that has T_{eff} values elevated 150–200 K from the low scale, as advocated by King (1993) and Axer et al. (1994). We used the low T_{eff} scale parameters here to tie more closely to previous abundance analyses of these stars (e.g., Pilachowski, Sneden, & Kraft 1996). Model parameters are given in Table 2.

We employed the iterated line lists with these model atmospheres to produce synthetic spectra for all stars and empirically smoothed these spectra to match the combined broadening effects of instrumental and stellar macro-turbulent spectral broadening. The abundances of all elements except Ag were initially set to match the metallicities [M/H] given in Table 2. Assumed abundances were altered until we achieved an acceptable match between the synthetic and observed spectra. The abundances of all elements except Ag were varied together with no allowance for possible small star-to-star relative abundance ([X/Fe]) varia-

tions. The abundances of iron (and other Fe-peak elements) that yielded the best overall fit to the observed spectra in the two wavelength regions are given in Table 2 in the columns labeled [Fe/H] 3280 and 3382 Å; the offsets from initial [M/H] are mostly ≈ 0.1 dex or less. After choosing the metallicity for the best average synthesis/observation match, the abundance of Ag was varied in trial syntheses. We show examples of the syntheses in Figure 2 (for the very metal-poor giant HD 2665) and Figure 3 (for the moderately metal-poor main sequence star HD 103095). The derived [Ag/Fe] ratios from each spectral region are entered in rightmost two columns of Table 2. To compute [Ag/Fe] from a line at 3280 or 3382 Å we used the estimated $\log \epsilon(\text{Ag})$ value from our spectrum, subtracted from it the corresponding $\log \epsilon(\text{Ag})$ derived above for the Sun to compute [Ag/H] for that line, and finally subtracted the [Fe/H] value derived for the surrounding spectral region.

We estimate that the abundance uncertainty from the comparison of synthetic and observed spectra (Ag I profile fitting and continuum placement errors) amounted to ± 0.10 in [Ag/Fe] for each star. An additional ± 0.1 dex

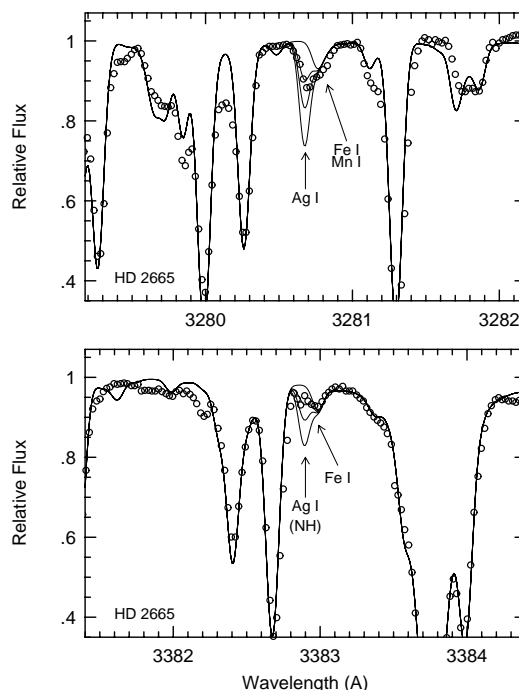


FIG. 2.—Observed spectra (circles) and synthetic spectra (four solid lines) of both Ag I lines in HD 2665. Only the assumed abundance of Ag was changed in the four syntheses, taking the values [Ag/Fe] = -12.0, -0.3, 0.0, and +0.3.

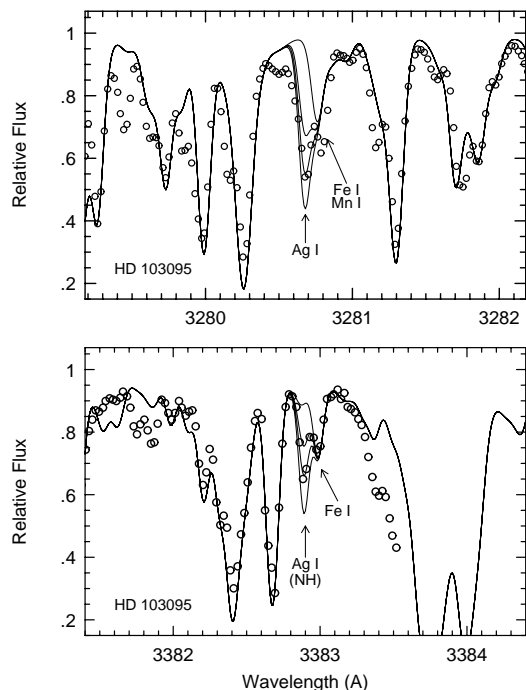


FIG. 3.—Observed synthetic spectra of the Ag I lines in HD 103095. The lines and symbols have the same meanings as in Fig. 2.

uncertainty arises from the $[\text{Fe}/\text{H}]$ estimates based on our spectra. The model atmosphere parameter uncertainties influencing $[\text{Ag}/\text{Fe}]$ are small. Many lines in these spectral regions that we used to estimate $[\text{Fe}/\text{H}]$ are Fe-peak neutral lines of moderate EP (~ 2.0 eV). Therefore we computed the variation of derived Ag abundance from the 0.0 eV Ag I lines under reasonable excursions in model parameter choices and compared those with the variation in derived iron abundance from a 2.2 eV Fe I line in the same wavelength region. These tests showed that $\delta[\text{Ag}/\text{Fe}] = \pm 0.01$ for $\delta T_{\text{eff}} = \pm 150$ K, $\delta[\text{Ag}/\text{Fe}] = \pm 0.09$ for $\delta \log g = \pm 0.3$, $\delta[\text{Ag}/\text{Fe}] = \pm 0.02$ for $\delta[M/\text{H}] = \pm 0.3$ (variation in assumed metallicity in computing a model atmosphere), $\delta[\text{Ag}/\text{Fe}] = \pm 0.08$ for $\delta v_t = \pm 0.25$ km s $^{-1}$. However, derived model atmosphere parameters usually are at least partly correlated. For example, higher assumed values of T_{eff} necessitate higher values of $\log g$ to maintain ionization equilibrium. Thus the errors in $[\text{Ag}/\text{Fe}]$ induced by model parameter errors are probably less than the collection of individual uncertainties listed here. However, to be conservative we accept ± 0.10 as an estimate of the dependence of $[\text{Ag}/\text{Fe}]$ on these parameters. Summing the three “internal” error sources given here in quadrature, the total uncertainty is $\delta[\text{Ag}/\text{Fe}] = \pm 0.17$. Finally, an “external” abundance scale error of about 0.1 dex probably exists due to the above-mentioned solar Ag abundance uncertainties, but that error source should not affect star-to-star $[\text{Ag}/\text{Fe}]$ comparisons.

4. DISCUSSION AND CONCLUSIONS

We have detected the resonance lines of Ag I in Keck I HIRES near-UV spectra of four halo stars in the metallicity range $-1.3 \geq [\text{Fe}/\text{H}] \geq -2.2$. Our model atmosphere synthetic spectrum analysis yields a mean Ag abundance in these stars of $\langle [\text{Ag}/\text{Fe}] \rangle = +0.22 \pm 0.06$. The quoted uncertainty is simply the standard deviation in the derived

abundances, and a more realistic uncertainty is probably ± 0.15 , from the discussion above. Silver abundance upper limits based on nondetection of the Ag I lines in three warmer and more metal-poor stars are not in conflict with this mean value.

There is no apparent trend with metallicity of $[\text{Ag}/\text{Fe}]$. In Figure 4 we plot $[\text{Ag}/\text{Fe}]$ abundances and upper limits as a function of $[\text{Fe}/\text{H}]$. For comparison, we also plot the mean abundances for several other neutron-capture elements reported in two recent abundance studies of metal-poor stars: Zhao & Magain (1991) and Gratton & Sneden (1994). The mean abundances are for stars of those studies in the metallicity range $-1.1 \geq [\text{Fe}/\text{H}] \geq -2.3$. The star-to-star scatters about each mean $[\text{X}/\text{Fe}]$ level are $\approx \pm 0.12$, and for Y and Zr, the mean abundances in these two studies agree to within 0.05 dex. For clarity in this figure, we have used only one line to depict the mean abundances of Y, La, and Ce, and one line for Sm and Dy, because the $[\text{X}/\text{Fe}]$ values of these elements are almost identical. We have not indicated abundance levels for easily observed Ba and Sr, because known analysis difficulties with the available (very strong) ionized lines of these elements render the mean levels of these elements less certain than the ones shown in Figure 4.

The mean relative abundances of the elements in this figure (including now Ag) roughly correlate with their expected neutron-capture origins. Burris et al. (1998) give a new tabulation of the fractional contribution of the r -process and s -process to each of these elements in solar system material. Their numbers update the table in Sneden et al. (1996), which is based on the extensive investigation of Käppeler et al. (1989). Their r/s breakdown suggests that the solar Ag abundance is “79% r -process,” meaning that the r -process must have dominated the synthesis of Ag in creating its solar system content; the s -process was responsible for only about 21% of the observed Ag. But the r -process has been a heavy contributor to the solar abundances of nearly all elements that have positive mean $[\text{X}/\text{Fe}]$ values in

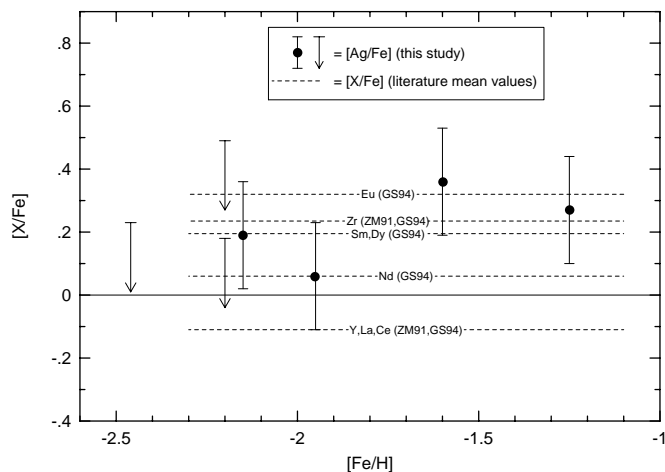


FIG. 4.—Relative abundances of Ag and other neutron-capture elements as functions of $[\text{Fe}/\text{H}]$ metallicity. The filled circles with error bars represent the abundances of four stars with detected Ag I lines, and the downward-pointing arrows represent the abundance upper limits of three stars with immeasurably weak Ag I lines. The horizontal dashed lines show mean levels of other neutron-capture elements in the metallicity range $-1.0 \geq [\text{Fe}/\text{H}] \geq -2.3$. These mean levels, labeled by element name and literature shorthand citation, are from two recent large-sample abundance studies of metal-poor stars: ZM91 = Zhao & Magain (1991), and GS94 = Gratton & Sneden (1994).

Figure 4. Burris et al. list Eu as 97% *r*-process in solar system material; Dy, 88%; Sm, 66%; and Nd, 53%. The only primarily *s*-process element of this group is Zr, at 19% *r*-process. However, all elements with negative $[X/Fe]$ values in Figure 4 are primarily *s*-process: Y, 28% *r*-process; La, 25%; and Ce, 19%.

These fractional solar system abundance contributions, together with the relative abundance ratios in these metal-poor stars, suggest simply that in the metallicity regime considered here, Ag synthesis was accomplished in the same *r*-process main component that produced relatively large amounts of Nd, Dy, and Eu early in the Galaxy, presumably in Type II SNe. With $[Ag/Fe]$ values determined in only four stars we have dealt with only mean abundance levels, but it is possible that $[Ag/Fe]$ correlates well on a star-by-star basis with $[X/Fe]$ of other *r*-process-dominant elements. Consider HD 2665 and HD 6755: from Table 2, the mean $[Ag/Fe]$ values are -0.01 and $+0.36$, respectively. Burris et al. (1998) have derived neutron-capture abundances for a large sample of metal-poor giant stars, and for HD 2665 they derive $[Nd/Fe] = +0.22$, $[Eu/Fe] = +0.23$, and $[Dy/Fe] = +0.28$; for HD 6755 these ratios are $+0.42$, $+0.50$, and $+0.52$. Thus, while the $[Ag/Fe]$ values of our study for these stars are about 0.2 dex lower than the abundances of other neutron-capture elements determined by Burris et al., the differences between the two stars are very similar. Obviously more detections of Ag I lines in stars of the Burris et al. sample are needed to substantiate or disprove this suggested correlation.

Our initial exploration of Ag abundances in metal-poor halo stars has shown no clear evidence for the existence of two different types of *r*-process events (as proposed by Wasserburg et al. 1996) in neutron-capture material of the

early Galaxy. However, our work must be considered as a beginning, not a definitive test. Recent abundance studies (e.g., McWilliam et al. 1995) have concluded that substantial departures from near-solar system abundance ratios for many element groups become noticeable only at metallicities less than $[Fe/H] \sim -2.5$. It will be of great interest to obtain Ag abundances in such “ultra-metal-poor” stars. We caution, however, that based on our nondetections of Ag I features in three stars, the ultra-metal-poor candidates for future Ag abundance probably must be giants with (approximately) $T_{\text{eff}} < 4800$ K, in order to enhance the overall spectrum line strengths. Unfortunately, this requirement emphasizes stars with low near-UV fluxes, so the observing time requirements will be large. Finally, candidates with the highest priority ought to be those ultra-metal-poor stars with substantial neutron-capture element levels, particularly the star CS 22892-052 (Sneden et al. 1996; $[Eu/Fe] \simeq +1.6$) and perhaps also HD 115444 (Griffin et al. 1982, Gilroy et al. 1988; $[Eu/Fe] \simeq +0.4$).

Thanks are given to Tom Bida for performing the service observations of HD 103095. J. R. K. and C. P. D. gratefully acknowledge support during the observations and data reduction from NASA grants HF-1046.01-93A and HF-1042.01-93A awarded by the Space Telescope Science Institute, which is operated by the Association of Universities for Research in Astronomy, Inc., under contract NAS 5-26555. C. P. D. also acknowledges with thanks support from the University of Hawaii Foundation through the Beatrice Watson Parrent Postdoctoral Fellowship. Additional support was provided by NSF grants AST 94-09793 to A. M. B., and AST 93-15068 and AST 96-18364 to C. S.

REFERENCES

- Axer, M., Fuhrmann, K., & Gehren, T. 1994, *A&A*, 291, 895
 Balachandran, S. C., & Bell, R. A. 1997, *BAAS*, 191, No. 74.08
 ———. 1998, *Nature*, 392, 791
 Boesgaard, A. M. 1996, in *ASP Conf. Ser. 92, Formation of the Galactic Halo ... Inside and Out*, ed. H. Morrison & A. Sarajedini (San Francisco: ASP), 327
 Burris, D. L., Pilachowski, C. A., Armandroff, T., Cowan, J. J., & Sneden, C. 1998, in preparation
 Carney, B. W. 1983, *AJ*, 83, 623
 Cowan, J. J., Thielemann, F.-K., & Truran, J. W. 1991, *Phys. Rep.*, 208, 267
 Deliyannis, C. P., Boesgaard, A. M., King, J. R., & Duncan, D. 1998, *AJ*, submitted
 Fitzpatrick, M. J., & Sneden, C. 1987, *BAAS*, 19, 1129
 Fuhr, J. R., & Wiese, W. L. 1996, in *CRC Handbook of Chemistry and Physics*, ed. D. R. Lide (Boca Raton, FL: CRC Press), 10-128
 Fuhrmann, K., Axer, M., & Gehren, T. 1995, *A&A*, 301, 492
 Gilroy, K. K., Sneden, C., Pilachowski, C. A., & Cowan, J. J. 1988, *ApJ*, 327, 298
 Gratton, R. G., & Sneden, C. 1994, *A&A*, 287, 927
 Green, E. M., Demarque, P., & King, C. R. 1987, *The Revised Yale Isochrones and Luminosity Functions* (New Haven: Yale Univ. Obs.)
 Grevesse, N. 1984, *Phys. Scr.*, T8, 49
 Grevesse, N., Noels, A., & Sauval, A. J. 1996, in *ASP Conf. Ser. 99, Cosmic Abundances*, ed. S. S. Holt & G. Sonneborn (San Francisco: ASP), 117
 Griffin, R., Griffin, R., Gustafsson, B., & Vieira, T. 1982, *MNRAS*, 198, 637
 Gustafsson, B., Bell, R. A., Erickson, K., & Nordlund, Å. 1975, *A&A*, 42, 407
 Hannaford, P., Lowe, R. M., Grevesse, N., Biémont, E., & Whaling, W. 1982, *ApJ*, 261, 736
 Holweger, H., & Müller, E. A. 1974, *Sol. Phys.*, 39, 19
 Käppeler, F., Beer, H., & Wisshak, K. 1989, *Rep. Prog. Phys.*, 52, 945
 King, J. R. 1993, *AJ*, 106, 1206
 Kurucz, R. L. 1993, CD-ROM 13, ATLAS9 Stellar Atmosphere Programs and 2 km/s Grid (Cambridge: Smithsonian Astrophys. Obs.)
 ———. 1995a, in *ASP Conf. Ser. 78, Astrophysical Applications of Powerful New Databases*, ed. S. J. Adelman & W. L. Wiese (San Francisco: ASP), 205
 ———. 1995b, in *ASP Conf. Ser. 81, Laboratory and Astronomical High Resolution Spectra*, ed. A. J. Sauval, R. Blomme, & N. Grevesse (San Francisco: ASP), 583
 Kurucz, R. L., Furenlid, I., Brault, J., & Testerman, L. 1984, *Solar Flux Atlas from 296 to 1300 nm* (Cambridge: Harvard Univ. Press)
 Kurucz, R. L., & Peytremann, E. 1975, *A Table of Semiempirical g_f Values*, (SAO Spec. Rep. 362) (Cambridge: Smithsonian Astrophys. Obs.)
 McWilliam, A. 1997, *ARA&A*, 35, 503
 McWilliam, A., Preston, G. W., Sneden, C., & Searle, L. 1995, *AJ*, 109, 275
 Meyer, B. S. 1994, *ARA&A*, 32, 153
 Moore, C. E., Minnaert, M. G. J., & Houtgast, J. 1966, *The Solar Spectrum 2935 Å to 8770 Å* (NBS Monogr. 61) (Washington: GPO)
 Pilachowski, C. A., Sneden, C., & Booth, J. 1993, *ApJ*, 407, 699
 Pilachowski, C. A., Sneden, C., & Kraft, R. P. 1996, *AJ*, 111, 1689
 Ross, J. E., & Aller, L. H. 1972, *Sol. Phys.*, 35, 281
 Ryan, S. G., Beers, T. C., Deliyannis, C. P., & Thorburn, J. A. 1996, *ApJ*, 458, 543
 Sneden, C. 1973, *ApJ*, 184, 839
 Sneden, C., McWilliam, A., Preston, G. W., Cowan, J. J., Burris, D. L., & Armosky, B. J. 1996, *ApJ*, 467, 819
 Sneden, C., & Parthasarathy, M. 1983, *ApJ*, 267, 757
 Tomkin, J., Lemke, M., Lambert, D. L., & Sneden, C. 1992, *AJ*, 104, 1568
 Vogt, S. S., et al. 1994, *Proc. SPIE*, 2198, 362
 Wallerstein, G., et al. 1997, *Rev. Mod. Phys.*, 69, 995
 Wasserburg, G. J., Busso, M., & Gallino, R. 1996, *ApJ*, 466, L109
 Wolf, S. C., & Wallerstein, G. 1967, *ApJ*, 150, 257
 Zhao, G., & Magain, P. 1991, *A&A*, 244, 425